ResearchGate

See discussions, stats, and author profiles for this publication at: https://www.researchgate.net/publication/231376034

Selective Absorption of H2S from a Gas Mixture with CO2 by Aqueous N-Methyldiethanolamine in a Rotating Packed Bed

ARTICLE *in* INDUSTRIAL & ENGINEERING CHEMISTRY RESEARCH · MAY 2010

Impact Factor: 2.59 · DOI: 10.1021/ie100678c

CITATIONS
16

READS
120

5 AUTHORS, INCLUDING:

Zhi Qian
Chinese Academy of Sciences
11 PUBLICATIONS **52** CITATIONS
SEE PROFILE

Lianbin Xu
Beijing University of Chemical Technology
37 PUBLICATIONS **763** CITATIONS
SEE PROFILE

Available from: Lianbin Xu
Retrieved on: 03 February 2016

Selective Absorption of H_2S from a Gas Mixture with CO_2 by Aqueous *N*-Methyldiethanolamine in a Rotating Packed Bed

Zhi Qian,[†] Lian-Bin Xu,[†] Zhen-Hu Li,[‡] Hua Li,[†] and Kai Guo*,[†]

Research Center of the Ministry of Education for High Gravity Engineering and Technology, Beijing University of Chemical Technology, Beijing 100029, PR China, and Beijing research institute of chemical industry, SINOPEC, Beijing 100013, PR China

In this work, selective absorption of H_2S from a gas mixture with CO_2 into *N*-methyldiethanolamine (MDEA) is investigated experimentally and theoretically in a rotating packed bed (RPB). In the RPB, various rotating speeds, gas flow rates, liquid flow rates, and concentrations of MDEA aqueous solutions were studied by means of the evaluation of removal efficiency, selectivity, and overall volumetric mass transfer coefficient. The reaction−diffusion mass transfer model based on penetration theory for the selective absorption process is developed, accordingly. The results of experiment and model show that the uppermost function of RPB in selective absorption of H_2S is to restrain the CO_2 removal efficiency but sharply intensify the absorption of H_2S. The mass transfer coefficient of CO_2 absorption is enhanced in RPB. However, the total amount of CO_2 mass transfer virtually is low because of the short gas−liquid contact time, small volume of packing, and large gas−liquid ratio within the RPB, and the CO_2 removal efficiency is merely around 9.50%. For the penetration of H_2S into liquid film, it is just 2.0×10^{-9} s that H_2S needs to be exhausted at 10^{-8} m into the liquid film. And the lifetime of a liquid film in the RPB is 7 orders of magnitude bigger than this penetration time of H_2S. So the reaction and mass transfer of H_2S still can be completed even at the very short gas−liquid contact time within the RPB, and a high H_2S removal efficiency of around 99.76% also can be achieved. In addition, a quantitative analysis based on the model, which suggests that the existence of CO_2 has little effect on the absorption of H_2S while the H_2S has an apparent negative impact on the absorption of CO_2, can be obtained for the selective absorption process. The experimental and model results have been found to be in a good agreement.

1. Introduction

Removal of acid gas components from gas mixtures containing CO_2 and H_2S is very important in natural gas processing and treating refinery off-gases and synthetic gases from coal and heavy oil gasification. In industrial gas processing, there is an increasing interest in gas absorption processes for the selective removal of H_2S from gas streams with a high ratio of CO_2 to H_2S. One motivation for this processing route is to increase the H_2S partial pressure in the regenerator off-gas to sulfur recovery unit (SRU). In the case of low heat-content fuel gas, H_2S must be removed for pipage and environmental reasons but CO_2 removal is not essential. Commercially, alkanolamines for the approach are monoethanolamine (MEA), diethanolamine (DEA), diisopropanolamine (DIPA), methyldiethanolamine (MDEA), and 2-amino-2-methyl-L-propanol (AMP). Among these alkanolamines, MDEA as an absorption solvent of acid gases is widely used today because it possesses characteristics such as higher H_2S selectivity, bigger absorption capacity, lower regeneration energy, smaller hot-degradation, and less corrosion.[1]

A selective treating process requires multiple stages and minimum contact time to avoid unwanted time dependent reactions. Compared with a conventional contactor, a rotating packed bed (RPB) is ideal for process operations that need both a "short" contactor and multiple stages.[2] The reaction of H_2S with MDEA is essentially instantaneous, and that of CO_2 with MDEA is slow relatively; so, a high selectivity for H_2S could be achieved in an RPB. Besides, the field of high gravity can prevent foaming and thus provide a more stable operation, and flooding does not occur up to ratios of gas flow rate to liquid flow rate higher than 1000 in RPB, so a high gas flow rate can be reached and a higher selectivity could be obtained correspondingly.

A few literature results on the selective removal of H_2S in aqueous solutions of MDEA in RPB have been reported.[2,3] Furthermore, a systematic experiment and quantitative description based on a model is still lacking. In this work, a comprehensive experiment upon the influence of various parameters on the selective absorption process in an RPB was carried out and the corresponding mass transfer model was established for quantitative analysis.

2. Theory

2.1. Reaction Scheme. For the reaction of CO_2 with MDEA, both the base catalysis mechanism[4] and the zwitterionic mechanism[5] are employed to explicitly explain the reaction processes.

The base catalysis mechanism is represented by

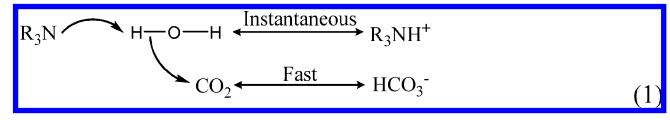

(1)

From the mechanism expression above, we can know that the rate-limiting step is

$$CO_2 + OH^- \xrightleftharpoons{k_{OH^-}} HCO_3^- \qquad (2)$$

* To whom correspondence should be addressed. Tel. and fax: +86-10-64448808. E-mail address: guok@mail.buct.edu.cn.
[†] Beijing University of Chemical Technology.
[‡] Beijing research institute of chemical industry, SINOPEC.

10.1021/ie100678c © 2010 American Chemical Society
Published on Web 05/18/2010

which is independent of and in parallel with the main reaction following the zwitterionic mechanism as follows:

$$CO_2 + R_3N \rightarrow R_3N{\cdot}CO_2 \quad (3)$$

$$R_3N{\cdot}CO_2 + H_2O \leftrightarrow R_3NH^+ + HCO_3^- \quad (4)$$

Combining eqs 3 and 4, we have the following:

$$CO_2 + R_3N + H_2O \xleftrightarrow{k_{2,MDEA}} R_3NH^+ + HCO_3^- \quad (5)$$

The reaction rate constant of CO_2 and MDEA is determined by previous research on the absorption of CO_2 into MDEA solution using a wetted wall column.[6,7] The liquid-film is the dominant resistance of CO_2 mass transfer.[8]

The reaction between H_2S and aqueous amines involves a proton transfer and is instantaneously fast with respect to mass transfer.[9] Everywhere in the liquid phase, including the interfacial liquid film, H_2S−MDEA equilibrium exists always.

$$R_3N + H_2S \leftrightarrow R_3NH^+ + HS^- \quad (6)$$

The CO_2−MDEA reaction is relatively slow compared with the CO_2−primary and CO_2−secondary amine reactions while the H_2S−MDEA reaction like all other amines is instantaneously fast, so a good H_2S selectivity could be expected with the tertiary amine.

2.2. Model for Mass Transfer of CO_2 and H_2S. Two models (1 and 2) established in this paper are based on three assumptions presented by Qian.[10] (1) The liquid flow in the RPB has been assumed to be laminar film flow on the packing surfaces. The majority of the liquid in the RPB exists in the form of a liquid film, and mass transfer takes place on it. (2) The surface areas of packing are regarded as the gas−liquid effective interfacial ones. (3) The rotor in the RPB consists of 31 layers of packing. The liquid film is renewed once every time it passes through one layer of packing. The mean lifetime of the liquid film in each layer is the same and determined by both liquid residence time and the total number of packing layers.

For model 1, it has been assumed that there is negligible interaction between the solute gases H_2S and CO_2 in the liquid phase for the selective absorption of the H_2S process. For model 2, the interaction between the H_2S and CO_2 in the liquid phase is taken into consideration.

Model 1: Without Interaction between H_2S and CO_2.

2.2.1. Absorption of CO_2 into MDEA in an RPB. The reaction between CO_2 and MDEA are following both the base catalysis and zwitterionic mechanisms, and the liquid film is the dominant resistance to CO_2 mass transfer. The absorption of CO_2 by aqueous solutions of MDEA in the RPB has been quantitatively described by a diffusion−reaction mass transfer model, and details about it are given elsewhere.[10]

2.2.2. Absorption of H_2S into MDEA in an RPB. The diffusion−reaction process for H_2S−MDEA mass transfer in a liquid film is modeled according to Higbie's penetration theory. The reaction between H_2S and MDEA is shown in eq 6, and equations describing the absorption of H_2S into MDEA solution are the following:

$$\frac{\partial c_{H_2S}}{\partial t} = D_{H_2S}\frac{\partial^2 c_{H_2S}}{\partial x^2} - k_{H_2S-MDEA}c_{MDEA}c_{H_2S} \quad (7)$$

$$\frac{\partial c_{MDEA}}{\partial t} = D_{MDEA}\frac{\partial^2 c_{MDEA}}{\partial x^2} - k_{H_2S-MDEA}c_{MDEA}c_{H_2S} \quad (8)$$

Thus, there are two partial differential equations which can be solved for the concentration distribution of H_2S and MDEA in the liquid film of packing. The reaction rate constant $k_{H_2S-MDEA}$ is around 10^9 m^3/(kmol s) (room temperature).[11] In fact, it is very hard to get exact value for $k_{H_2S-MDEA}$; if the magnitude of $k_{H_2S-MDEA}$ is close to the true value, it can meet the requirement of quantitative calculation. So 1×10^9 m^3/(kmol s) is taken for $k_{H_2S-MDEA}$ in this paper.

Initial and Boundary Conditions for Model 1. At $t = 0$ ($x \geq 0$) and $x \rightarrow \infty$ ($t \geq 0$), the concentration of H_2S is equal to zero because of the existence of instantaneous reaction[8] and that of MDEA is equal to its liquid bulk concentration.

$$C_{H_2S} = 0 \quad \text{and} \quad C_{MDEA} = C_{MDEA,BL} \quad (9)$$

At $x = 0$ (gas−liquid interface), the flux of the nonvolatile chemical specie is equal to zero, which leads to the following equation:

$$\frac{\partial c_{MDEA}}{\partial x} = 0 \quad x = 0, t > 0 \quad (10)$$

For the volatile component H_2S, the mass transfer rate in the gas near the interface is equal to the mass transfer rate in the liquid near the interface

$$-D_{H_2S}\frac{\partial c_{H_2S}}{\partial t} = k_{g,H_2S}[P_{H_2S} - H_{H_2S}c_{H_2S}(0,t)] \quad x = 0, t > 0 \quad (11)$$

So, the real partial pressure (or concentration) of H_2S at interface can be obtained

$$c_{H_2S}(0,t) = \frac{\left(P_{H_2S} - \dfrac{-D_{H_2S}}{k_{g,H_2S}}\dfrac{\partial c_{H_2S}}{\partial t}\right)}{H_{H_2S}} \quad x = 0, t > 0 \quad (12)$$

The diffusion process of H_2S at the gas−liquid interface can be regarded as pure H_2S diffusion.[12] For the case of pure gas H_2S in the gas phase, the interfacial partial pressure of the gas, $P^*_{H_2}S$ is the same as the bulk partial pressure of the gas, $P^*_{H_2}S$, and there is no mass transfer resistance in the gas phase. Hence, the boundary condition for gas H_2S at the gas−liquid interface is

$$c_{H_2S}(0,t) = c^*_{H_2S} = \frac{P_{H_2S}}{H_{H_2S}} \quad x = 0, t > 0 \quad (13)$$

To move the calculation result closer to the practical situation, the boundary condition near the interface is improved in this study. Both gas and liquid film resistances are important for H_2S absorption,[12,13] so the boundary condition should be modified, accordingly. The iteration method is employed to approach the real partial pressure of H_2S at the interface. First, the value of eq 13 as initial value is substituted into the model to get the concentration distribution of H_2S in the liquid film (c_{H_2S}). Then the c_{H_2S} is substituted into eq 12 to get the $c_{H_2S}(0,t)$. Finally, comparing the $c_{H_2S}(0,t)$with the initial value, if there is agreement, the initial value is regarded as real partial pressure of H_2S at the interface; if not, the $c_{H_2S}(0,t)$ as a new initial value is calculated again as per the above procedure until convergence.

Model 2: With Interaction between H_2S and CO_2. 2.2.3. Simultaneous Absorption of H_2S and CO_2 into MDEA Solutions in an RPB. According to the study of Ko,[7] the reaction between CO_2 and MDEA can be also regarded as an irreversible process and the modeling on the diffusion−reaction process can be simplified. In model 2, the interaction between H_2S and CO_2 is taken into consideration and the irreversible reaction for whole system is assumed. Higbie's penetration theory also is used to set up the diffusion−reaction partial differential equations which describe the simultaneous absorption of H_2S and CO_2 into MDEA solutions as follows:

$$\frac{\partial c_{H_2S}}{\partial t} = D_{H_2S}\frac{\partial^2 c_{H_2S}}{\partial x^2} - k_{H_2S-MDEA}c_{MDEA}c_{H_2S} \quad (14)$$

$$\frac{\partial c_{CO_2}}{\partial t} = D_{CO_2}\frac{\partial^2 c_{CO_2}}{\partial x^2} - \left(k_{CO_2-MDEA}c_{MDEA} + k_{CO_2-OH^-}\sqrt{\frac{K_w}{K_p}c_{MDEA}}\right)c_{CO_2} \quad (15)$$

$$\frac{\partial c_{MDEA}}{\partial t} = D_{MDEA}\frac{\partial^2 c_{MDEA}}{\partial x^2} - k_{H_2S-MDEA}c_{MDEA}c_{H_2S} - \left(k_{CO_2-MDEA}c_{MDEA} + k_{CO_2-OH^-}\sqrt{\frac{K_w}{K_p}c_{MDEA}}\right)c_{CO_2} \quad (16)$$

The loading of CO_2 in amine is relatively small because of the high selectivity of MDEA solution, so the OH^- concentration can be estimated from the relation given by Astarita.[14]

$$\sqrt{\frac{K_w}{K_p}c_{MDEA}} = c_{OH^-} \quad (17)$$

where K_w and K_p are the water dissociation constant and MDEA protonation constant, respectively. There are three partial differential equations for the process of simultaneous absorption of H_2S and CO_2, which can be solved for the concentrations of H_2S, CO_2, and MDEA in the liquid film. Consequently, the interaction between H_2S and CO_2 can be quantified.

Initial and Boundary Conditions for Model 2. At $t = 0$ ($x \geq 0$) and $x \rightarrow \infty$ ($t \geq 0$), the concentrations of all chemical species are equal to their liquid bulk concentrations:

$$c_i = 0, c_3 = c_{3,BL}, i = 1, 2, 3 \quad (18)$$

Here, $c_1 = H_2S$, $c_2 = CO_2$, and $c_3 =$ MDEA.

Besides, the mass transfer rate of MDEA at $x \rightarrow \infty$ is equal to the sum of that of H_2S and CO_2 at $x = 0$:

$$D_3\left.\frac{\partial c_3}{\partial x}\right|_{x=\infty} = D_1\left.\frac{\partial c_1}{\partial x}\right|_{x=0} + D_2\left.\frac{\partial c_2}{\partial x}\right|_{x=0} \quad (19)$$

At $x = 0$ (gas−liquid interface), the flux of the nonvolatile chemical species is equal to zero, which leads to the following equation:

$$\frac{\partial c_3}{\partial x} = 0 \quad x = 0, t > 0 \quad (20)$$

For the volatile components c_1 and c_2, the mass transfer rate in the gas near the interface is equal to the mass transfer rate in the liquid near the interface

$$-D_i\frac{\partial c_i}{\partial t} = k_{g,i}[P_i - H_i c_i(0,t)] \quad x = 0, t > 0 \quad (21)$$

So the real partial pressure (or concentration) of component i at the interface can be obtained

$$c_i(0,t) = \frac{\left(P_i - \frac{-D_i}{k_{g,i}}\frac{\partial c_i}{\partial t}\right)}{H_i} \quad x = 0, t > 0 \quad (22)$$

The diffusion process of gas i on the gas−liquid interface can be regarded as pure gas i diffusion.[12] For the case of pure gas i in the gas phase, the interfacial partial pressure of the gas, P_i^*, is the same as the bulk partial pressure of the gas, P_i^*, and there is no mass transfer resistance in the gas phase. Hence, the boundary condition for gas i at the gas−liquid interface is

$$c_i(0,t) = c_i^* = \frac{P_i}{H_i} \quad x = 0, t > 0 \quad (23)$$

The iteration method is also employed to approach the real partial pressure of component i at the interface; refer to the boundary conditions for model 1 for the details of the algorithm.

2.2.4. Method of Solution. The finite element method (FEM) based on the variation principle is employed to numerically solve the diffusion−reaction partial differential equations—models 1 and 2. The FEM is a powerful technique for finding the approximate solution of a partial differential equation where the domain boundaries of the given problem are so complex that standard methods such as the finite difference method (FDM) may have difficulties or even fail. A procedure is compiled in Flex PDE to solve the partial differential equations, and the concentration distributions of H_2S and MDEA in liquid film can be obtained. The program will converge in 5 min.

On the basis of the numerical solution to partial differential equations of model 1, Figure 1 presents the concentration distribution of H_2S in liquid film. Both X and Y axes are dimensionless, and they represent the penetration depth and liquid film lifetime, respectively. The Z axis denotes the concentration of H_2S, in moles per liter. The penetration depth of H_2S in the liquid film can be quantitatively figured out and is also clearly reflected in Figure 1. For the absorption of H_2S by 10% MDEA at the operation condition of a rotating speed of 1100 r/min and 293 K, the H_2S penetration length in the liquid film is around 1.0×10^{-8} m and the time needed to establish a steady concentration gradient, which means that the penetration depth of H_2S no longer varies with time, is also obtained, about 2.0×10^{-9} s.

On the basis of the numerical solution to the partial differential equations of model 2, Figures 2−4 show the concentration profiles in the liquid film for H_2S, CO_2, and MDEA, respectively. In Figures 2and 3, X and Y represent the penetration depth and penetration time, respectively. In Figure 4, the X and Y axes represent the penetration depth of MDEA from the liquid bulk to the liquid film and liquid film lifetime on packing, respectively. The Z axis denotes the concentration, in moles per liter. It is can be seen clearly that the H_2S concentration changes little compared to the case in model 1, which indicates that the existence of CO_2 has little effect on H_2S absorption in the RPB. According to the quantitative calculation, the penetration length of CO_2 is 2.0×10^{-5} m and the time needed to setup a steady concentration gradient is 1 s for the simultaneous absorption of H_2S and CO_2 by 10% MDEA at the operation conditions of a rotating speed of 1100 r/min

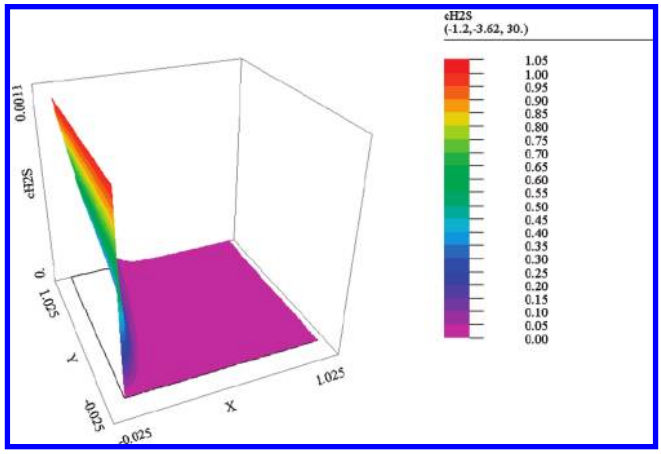

Figure 1. Concentration profile of H_2S in the liquid film. The maximum absolute value is 1.0×10^{-7} m on the *X* axis (dimensionless) and 5.0×10^{-9} s on the *Y* axis (dimensionless).

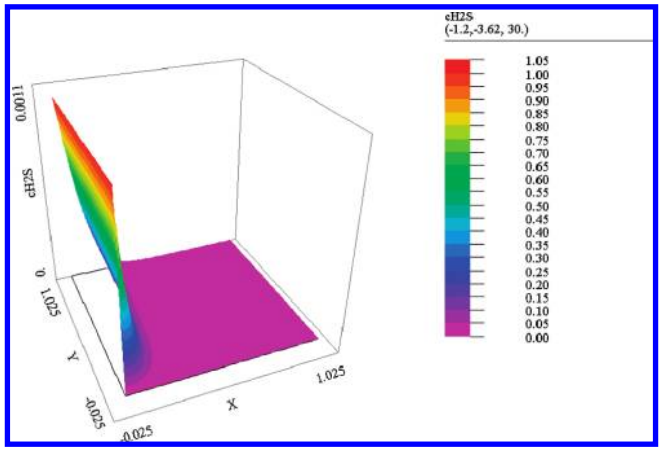

Figure 2. Concentration profile of H_2S in the liquid film. The maximum absolute value is 1.0×10^{-7} m on the *X* axis (dimensionless) and 5.0×10^{-9} s on the *Y* axis (dimensionless).

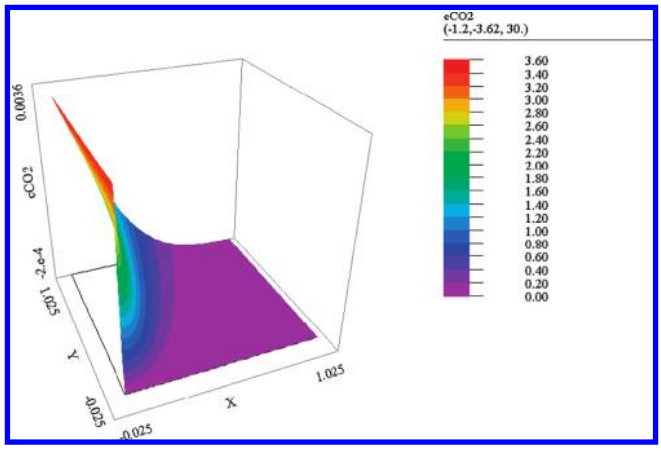

Figure 3. Concentration profile of CO_2 in the liquid film. The maximum absolute value is 5.0×10^{-5} m on the *X* axis (dimensionless) and 1 s on the *Y* axis (dimensionless).

and 293 K. Comparing the H_2S penetration process with that of CO_2, the penetration depth of H_2S is just $1/(2 \times 10^3)$ of that of CO_2, and the time needed to establish a steady concentration gradient of H_2S is just $1/(5 \times 10^8)$ that of CO_2. The steady mass transfer of H_2S has been completed when the CO_2 begins to penetrate. So it is also reasonable to conclude that the CO_2 absorption hardly exerts any impact on the H_2S absorption in the liquid film. For validating the conclusion based on model

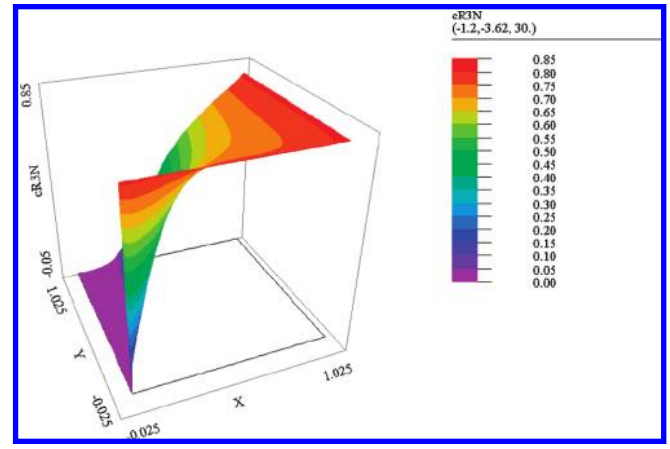

Figure 4. Concentration profile of MDEA in the liquid film. The maximum absolute value is 5.0×10^{-5} m on the *X* axis (dimensionless) and 0.015 s on the *Y* axis (dimensionless).

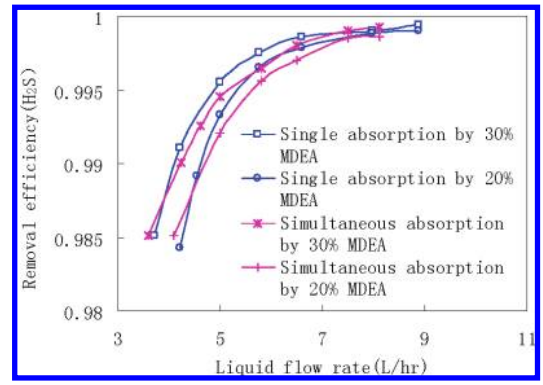

Figure 5. Comparison of H_2S removal efficiency between single absorption of H_2S and selective absorption of H_2S with CO_2 into 30% MDEA.

2, experiments with H_2S alone and both H_2S and CO_2 coexisting for absorption by MDEA were performed, and the comparison between the two cases is made as shown in Figure 5. The marginal difference between single absorption (H_2S) and simultaneous absorption (H_2S, CO_2) is observed in Figure 5.

On the other hand, the negative effect from the existence of H_2S on CO_2 absorption is apparent. For single absorption of CO_2 by MDEA, the reaction between CO_2 and MDEA is not instantaneous, so CO_2 cannot consume most of the MDEA in the liquid film. Furthermore, MDEA has enough time to diffuse from the liquid bulk into the liquid film. The reaction between CO_2 and MDEA can be regarded as the fast pseudo-first-order reaction,[7] and the concentration of MDEA is constant in the liquid film, i.e., the diffusion of MDEA in the liquid film is negligible. However, the MDEA concentration distribution in the liquid film is formed because of the instantaneous reaction between H_2S and MDEA, and then, the reaction between CO_2 and MDEA cannot be regarded as fast pseudo-first-order any more, i.e., the diffusion of MDEA exists in the liquid film. As shown in Figure 4, the concentration distribution of MDEA in the liquid film is different from that for single absorption of CO_2 by MDEA, which means that CO_2 has less chances to react with MDEA and the absorption of CO_2 will be restrained consequently. In this case, the reaction between CO_2 and MDEA is second-order, and the diffusion of MDEA in the liquid film must be taken into consideration to model the CO_2 absorption process with the existence of H_2S. For the H_2S absorption process, whether the CO_2 exists or not does not matter a lot and both models 1 and 2 can describe the absorption of H_2S by MDEA solutions. For the CO_2 absorption process, the existence

of H_2S has a negative effect on the CO_2 absorption and the interaction between H_2S and CO_2 in the liquid phase must be considered, so only model 2 can quantitatively depict this process.

2.2.5. Mass Transfer Coefficient and Mass Balance in the High Gravitational Field. For an RPB, the liquid film is renewed when it passes through the packing layer and the renewal frequency is determined by

$$S = u\frac{N_S}{R_1 - R_2} \tag{24}$$

where N_S is the number of layers of the wire-meshed packing, 31 in this study, while R_2 and R_1 are the outer and inner radii of the packing, respectively. The term u is the average radial flow rate of the liquid film:[15]

$$u = 0.02107L^{0.2279}(\omega R)^{0.5448} \tag{25}$$

where L is liquid flux. Then, the mean lifetime of the liquid film can be obtained via

$$\bar{t} = \frac{R_1 - R_2}{0.02107L^{0.2279}(\omega R)^{0.5448}N_S} \tag{26}$$

The time-averaged rate of absorption of H_2S and CO_2 per unit interfacial area is then expressed from the following equation

$$\bar{N}_i = \int_0^{\bar{t}} -D_i \left.\frac{\partial c_i}{\partial x}\right|_{x=0} \frac{1}{\bar{t}}\,\mathrm{d}t, \quad i = \mathrm{H_2S}, \mathrm{CO_2} \tag{27}$$

Then the liquid-side mass transfer coefficient in the high gravitational field can be obtained by

$$k_{L,i} = \frac{\bar{N}_i}{(c_i^* - c_i^0)}, \quad i = \mathrm{H_2S}, \mathrm{CO_2} \tag{28}$$

CO_2 absorption is controlled by diffusion with fast chemical reactions, and gas film resistance is never significant for CO_2 absorption. For H_2S absorption, both gas and liquid film resistances are important.[12,13] Previous study reported that the values of gas-side mass transfer coefficient (k_G) in an RPB lie in a range similar to those in a static absorption plant.[16] Hence, the gas-phase resistance to mass transfer was determined by experiments of absorption of H_2S into 10% aqueous hydroxide solutions from a 1% H_2S−99% N_2 gas mixture as described by Savage et al.[17]

The gas-phase mass transfer coefficient (K_{G,H_2S}) of the RPB for H_2S absorption can be determined by the following equation:

$$\frac{1}{K_{G,H_2S}} = \frac{1}{k_{G,H_2S}} + \frac{H_{H_2S}}{k_{L,H_2S}} \tag{29}$$

Considering an element of the RPB with radial length dR, differential mass balance equations for H_2S and CO_2 can be given as:

$$K_{G,H_2S}\frac{8.314}{101.325}TP\alpha(y_{H_2S} - y^*_{H_2S})2\pi hR\,\mathrm{d}R = G_{N_2}\,\mathrm{d}\left(\frac{y_{H_2S}}{1 - y_{H_2S}}\right) \tag{30}$$

$$K_{L,CO_2}\frac{8.314}{101.325}T\frac{P}{H}\alpha(y_{CO_2} - y^*_{CO_2})2\pi hR\,\mathrm{d}R = G_{N_2}\,\mathrm{d}\left(\frac{y_{CO_2}}{1 - y_{CO_2}}\right) \tag{31}$$

Where y_i and y_i^* represent mole fraction of component i in the gas bulk and that of component i in equilibrium with the bulk liquid, respectively. P denotes total pressure. Since the reaction of H_2S with amine is instantaneously fast, the value of $yH2^*_S$ can be assumed to be zero approximately.[8] Besides, according to accurate solution to a nonlinear equilibrium equation set,[6] it was proven that the concentration of free CO_2 in the liquid bulk was so marginal that the corresponding equilibrium mole fraction in the gas phase $y^*_{CO_2}$ could be negligible. Integrating the above equations from gas inlet (R_{in}) to outlet (R_{out}) for H_2S and CO_2 gives the following equations:

$$y_{H_2S,out} = \frac{1}{\dfrac{1 - y_{H_2S,in}}{y_{H_2S,in}}\exp\left[\dfrac{K_{G,H_2S}0.082TP\alpha\pi h(R_{out}^2 - R_{in}^2)}{G}\right] + 1} \tag{32}$$

$$y_{CO_2,out} = \frac{1}{\dfrac{1 - y_{CO_2,in}}{y_{CO_2,in}}\exp\left[\dfrac{K_{L,CO_2}0.082T\dfrac{P}{H_{CO_2}}\alpha\pi h(R_{out}^2 - R_{in}^2)}{G}\right] + 1} \tag{33}$$

2.3. Evaluation of Absorption Performance. To evaluate the H_2S and CO_2 absorption performance of the RPB, the overall volumetric mass transfer coefficient (K_Ga) is determined by the following equation.[18]

$$K_Ga = \frac{G}{\pi h(R_{out}^2 - R_{in}^2)}\ln\left(\frac{y_{i,in}}{y_{i,out}}\right) \tag{34}$$

The selectivity of amine solvents for H_2S has been defined by previous workers[17] as the tendency for the ratio of H_2S to CO_2 contents to be larger in the liquid phase than they are in the gas phase. The selectivity factor is used as a yardstick for the H_2S selectivity, and the value of selectivity factor is expressed as

$$S = \frac{\alpha_{H_2S} - \alpha'_{H_2S}}{y_{H_2S}}\Bigg/\frac{\alpha_{CO_2} - \alpha'_{CO_2}}{y_{CO_2}} \tag{35}$$

The value of H_2S and CO_2 removal efficiency are calculated by the following equation based on a material balance:

$$\eta_{H_2S} = 1 - \frac{y'_{H_2S}}{y_{H_2S}}\frac{1 - y_{H_2S} - y_{CO_2}}{1 - y'_{H_2S} - y'_{CO_2}} \tag{36}$$

$$\eta_{CO_2} = 1 - \frac{y'_{CO_2}}{y_{CO_2}}\frac{1 - y_{H_2S} - y_{CO_2}}{1 - y'_{H_2S} - y'_{CO_2}} \tag{37}$$

where y_i and y'_i denote the inlet and outlet mole fraction of component i, respectively.

3. Experimental Section

The RPB employed in this study had an inner diameter of 42 mm, an outer diameter of 146 mm and a height of 20 mm,

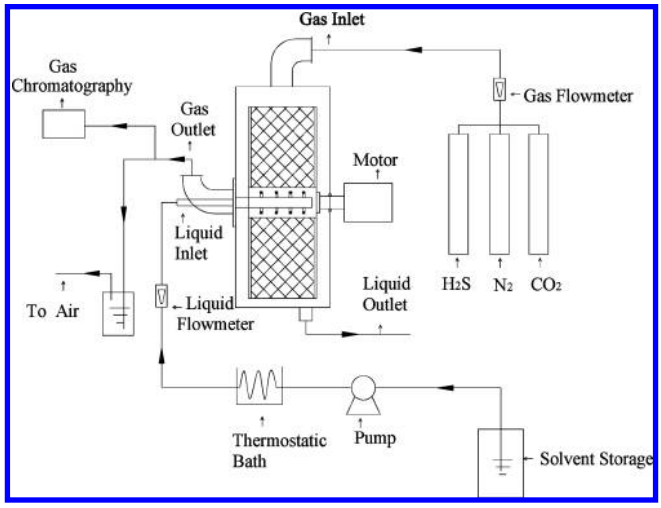

Figure 6. Experimental flowchart for the selective absorption of H_2S into MDEA in the RPB.

as shown in Figure 6. The stainless wire mesh was used as the packing with a specific area of 550 m^2/m^3 and a voidage of 97%. The total volume of the packing was 307 cm^3. The packing consists of 31 layers. The gas stream containing H_2S, CO_2, and N_2 at a mole radio of 1:10:89 flowed inward from the outer edge of the RPB by pressure, and the aqueous absorbent was sprayed onto the inner edge of the RPB via a distributor. The aqueous absorbent moved outward and left from the outer edge of the RPB by centrifugal force. The composition of feed gas was determined from the respective flow rates. H_2S and CO_2 in the gas stream were dissolved and reacted with MDEA while gas and liquid contacted countercurrently in the RPB. The inlet gas had a flow rate of 1100 L/h. The rotating speed varied from 600 to 1300 r/min. For all runs, a steady state operation was reached within 2 min. The H_2S and CO_2 concentrations in the inlet and outlet gas streams were measured by gas chromatograph (SP-2100, BAIF Chromatograph Instrument Center). CO_2 mole fraction ranged from 0 to 10% and those of H_2S from 0 to 1% (0−10 000 ppm). The operation temperatures were maintained at 293, 303, and 313 K, respectively, via thermostatic bath, and the pressure was ambient pressure. The aqueous solutions of MDEA were prepared by distilled−deionized water, and the concentration of MDEA in the solutions was determined by titration with HCl. All the experiments were conducted in the concentration range of 10−30 mass % MDEA. The H_2S loading of the amine solution was determined by titration with a standard $AgNO_3$ solution.[19] For the determination of CO_2 content of the liquid, the volume method was employed.[9]

4. Results and Discussion

4.1. Effect of Rotating Speed on Absorption Performance. In this section, MDEA aqueous solutions with mass concentrations from 10% to 30% and liquid flow rates of 6.1 L/h entered into the RPB and contacted the gas mixed stream with a gas flow rate of 500 L/h countercurrently. Figure 7 shows the dependence of K_Ga on the rotating speed, it is also seen that K_Ga is increased with an increase in the rotating speed in the range of 500−1100 rpm, indicating that the mass-transfer resistances are reduced with an increase in the rotating speed. However, when the rotating speed was further increased, a reverse effect on K_Ga is observed. This is probably due to the fact that the extent of reduction in mass transfer resistances at higher rotating speed is compensated by a reduction of the retention time that is unfavorable to chemical absorption.

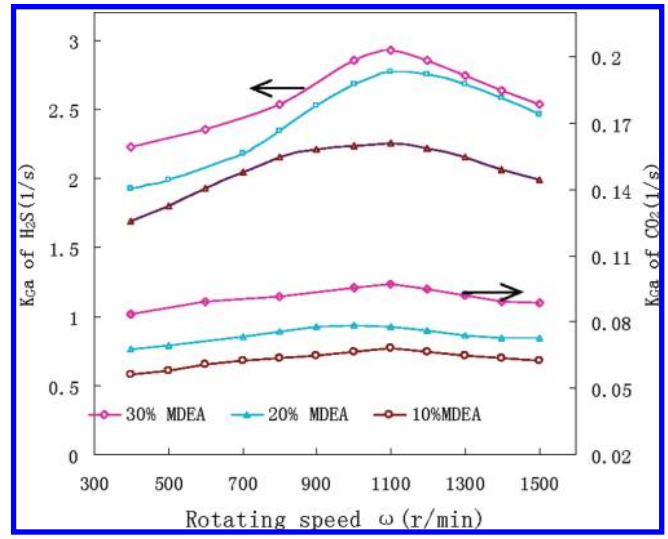

Figure 7. Effects of rotating speed on overall volumetric mass transfer coefficient (K_Ga).

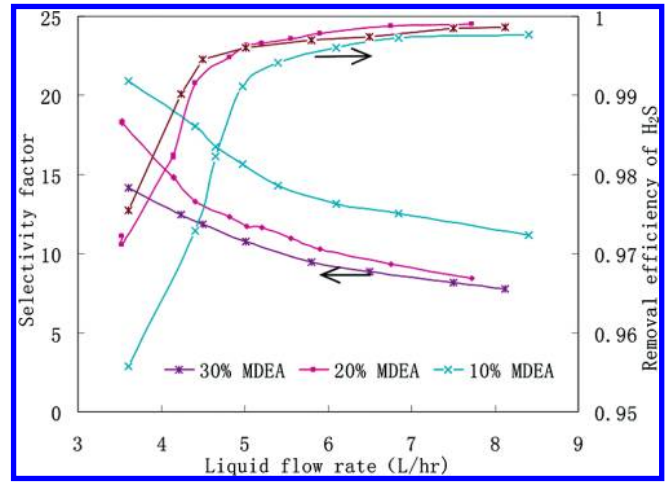

Figure 8. Effect of liquid flow rate on H_2S removal efficiency and selectivity factor.

Furthermore, the trend line of K_Ga for CO_2 absorption has less variation range compared to the H_2S as shown in Figure 7. This could be attributed to the existence of H_2S restraining the absorption of CO_2 and less chance for CO_2 to react with MDEA as pointed by the result of model analysis in section 2. The intensification for CO_2 absorption from RPB is compensated by a reduction of reaction rate leading the removal efficiency of CO_2 in a relatively stable state. Therefore, the observation suggests that the rotating speed of 1100 r/min be required to get a high H_2S removal efficiency and selectivity in the RPB for this paper.

4.2. Effect of Liquid Flow Rate and Amine Concentration on Absorption Performance. In this experiment, the MDEA concentration and liquid flow rate were respectively varied from 10% to 30% and 3.5 to 9 L/h under a rotating speed of 1100 r/min, temperature of 293 K, and gas flow rate of 500 L/h. Figure 8 shows that the H_2S removal efficiency rises with the increase in the liquid flow rate, while the selectivity factor shows in a reverse trend. Besides, it can be observed that the slope of the H_2S removal efficiency line is relatively large when the liquid flow rate is less than 5.3 L/h and the removal efficiency maintains a high level with a liquid flow rate more than 5.3 L/h. This is probably due to the fact that an even distribution of liquid on the packing can be formed when the liquid flow

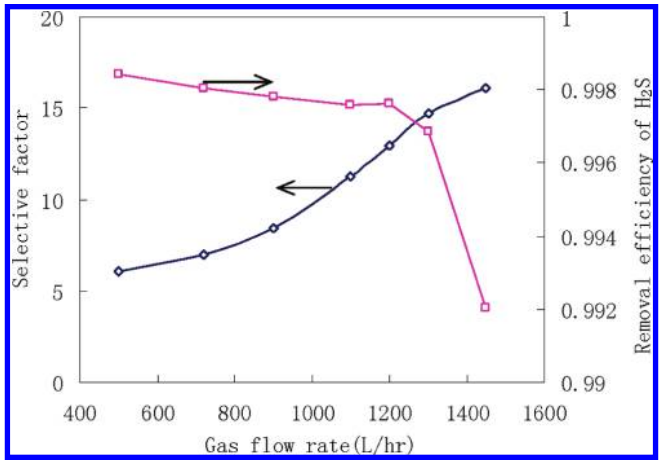

Figure 9. Effect of gas flow rate on H_2S removal efficiency and selectivity factor.

rate is more than 5.3 L/h and a steady effective gas−liquid mass transfer interface for favorable gas−liquid contact can be achieved. So it is essential to set a reasonable liquid flow rate so as to ensure a high H_2S removal efficiency and appropriate selectivity factor. On the basis of analysis of Figure 8, the liquid flow rate of 5.3 L/h is a modest operation condition to obtain an optimum result for this work. Figure 8 also depicts the variation of the H_2S removal efficiency with the MDEA mass concentrations in the range of 10−30%. Both the H_2S and CO_2 removal efficiencies improve with the increase in MDEA mass concentration. The reaction rate for H_2S−MDEA changes little with an increase in MDEA mass concentration because it is an instantaneous reaction, while the reaction rate for CO_2−MDEA changes a lot, and the existence of H_2S will lightly reduce the negative impact on the absorption of CO_2. So the variation range of H_2S removal efficiency is smaller than that of CO_2 and the selectivity factor of H_2S decreases with the rise in MDEA mass concentration. By analysis, 20% MDEA is the best mass concentration for H_2S selective absorption to achieve a relatively high H_2S removal efficiency and selectivity.

4.3. Effect of Gas Flow Rate on Absorption Performance. As shown in Figure 9, with increase in the gas flow rate in the range 500−1200 L/h, the removal efficiency of H_2S declines gently. When the gas flow rate is above 1200 L/h, the removal efficiency of H_2S reduces sharply compared to the case of a gas flow rate in the range 500−1200 L/h. While an increase in the gas flow rate could result in a reduction of the gas-side mass transfer resistance that would be beneficial to absorption, a decrease in contact time with the gas flow rate increasing would hinder the chemical absorption. From the obtained results, it is seen that the contact time also exhibits a greater effect on H_2S removal for the system when the gas flow rate is big enough. So, a gas flow rate over 1200 L/h should be avoided for obtaining a removal efficiency of H_2S as high as 99.8% (20 ppm) and a selectivity factor up to 13. Combining the appropriate fluid flow rate on the basis of the previous analysis with the gas flow rate of 1200 L/h, the optimum gas−liquid radio of 226 can be concluded for this experiment.

4.4. Effect of Temperature on Absorption Performance. The experimental results of effects of temperature on the overall volumetric mass transfer coefficients K_Ga of CO_2 and H_2S, removal efficiency of H_2S, and selectivity for aqueous MDEA solution are presented in Figures 10 and 11 along with their predicted values based on the model developed in this work.

It is observed that with the rise in temperature from 293 to 333 K the overall volumetric mass-transfer coefficient of H_2S

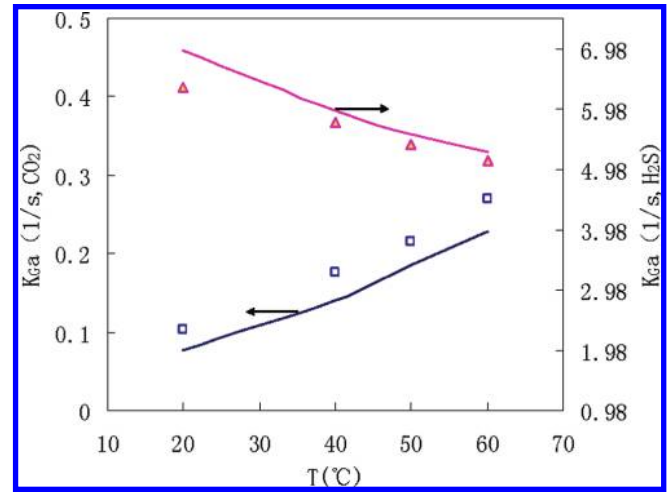

Figure 10. Effect of temperature on overall volumetric mass transfer coefficient (K_Ga).

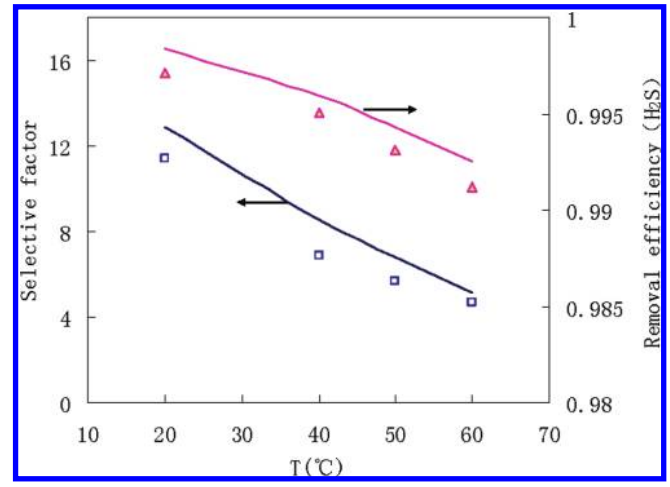

Figure 11. Effect of temperature on H_2S removal efficiency and selectivity factor.

decreases slowly, while the rate of absorption of CO_2 increases, resulting in a decrease in the selectivity factor for MDEA. Similar observations were reported earlier by Ouwerkerk[20] for absorption of H_2S in aqueous MDEA. Ouwerkerk[20] found that the rate of absorption was lower at higher temperature for low H_2S partial pressures (up to about 5.33 kPa). He concluded that, at low H_2S partial pressures, the effect of temperature on the equilibrium loading of the amine at the interface dominates the absorption of H_2S in amine. As shown in Figures 10 and 11, the experimental and model predicted results are in a good agreement. It is suggested that the high temperature has a significant effect on the reaction rate constant for the CO_2 absorption and Henry constant for H_2S absorption from the quantitative calculation based on the model. So, it is necessary to avoid a high operation temperature so as to ensure a high H_2S removal efficiency and selectivity factor.

5. Conclusions

The uppermost function of RPB in selective absorption of H_2S is to restrain the CO_2 removal efficiency but sharply intensify the absorption of H_2S. When CO_2 penetrates into the liquid film of MDEA solution, it needs more than 1 s to setup a steady concentration gradient and the liquid film lifetime in the RPB is merely 0.015 s. So the mass transfer process of CO_2 in the RPB is dynamic, and the shorter the liquid film lifetime,

the bigger the mass transfer coefficient. Although the mass transfer coefficient of CO_2 absorption is enhanced in the RPB, the total virtual amount of CO_2 mass transfer is low because of the short gas−liquid contact time, small volume of packing, and large gas−liquid ratio within the RPB and the CO_2 removal efficiency is merely around 9.50%. For the penetration of H_2S into liquid film, it is just 2.0×10^{-9} s that H_2S needs to be exhausted at 10^{-8} m into the liquid film. And the lifetime of the liquid film in the RPB is 7 orders of magnitude bigger than this penetration time of H_2S. So, the reaction and mass transfer of H_2S still can be completed even at the very short gas−liquid contact time within the RPB, and a high H_2S removal efficiency of around 99.76% also can be achieved. Finally, the conclusion can be resonably drawn that the properties of longer gas−liquid contact time, bigger packing volume, and smaller gas−liquid ratio belonging to a traditional packed bed are not the main reasons for high H_2S removal efficiency but for low selectivity and high CO_2 removal efficiency in the process of selective H_2S removal.

Acknowledgment

The financial support provided by National Basic Research Program of China (Grant No. 2009BC219903) and China Petroleum & Chemical Corporation (Grant No. 105044) are gratefully acknowledged.

Note Added after ASAP Publication: This paper was published on the Web on May 18, 2010, with the incorrect artwork for Figure 8. The corrected version was reposted on May 27, 2010.

Nomenclature

D = diffusivity, m^2/s
G = volumetric flow rate of gas, m^3/s
G_{N_2} = flow rate of N_2, m^3/s
h = height of packing, m
H = solubility of gas in solution, (kPa m^3)/kmol
$k_{2,MDEA}$ = second-order reaction rate constant, $m^3/(kmol\ s)$
k_G = gas-phase mass transfer coefficient, m/s
k_L = liquid-phase mass transfer coefficient, m/s
k_{OH^-} = reaction rate constant for CO_2 hydration, $m^3/(kmol\ s)$
L = liquid flux, m/s
$\bar{N}_i$ = time-averaged mass transfer rate of i per unit interfacial area, $kmol/(m^2\ s)$
P_i = partial pressure of i in the gas phase, kPa
P_i^* = partial pressure of i in the gas phase at the gas−liquid interface, kPa
Q = volumetric flow rate of the liquid, m^3/s
r = reaction rate, $kmol/(m^3\ s)$
R = geometrical mean radius
R_{out} = outer radius of rotator in the RPB, m
R_{in} = inner radius of the rotator in the RPB, m
$\bar{t}$ = mean lifetime of the liquid film, s
T = temperature, K
x = penetration depth, m
y = mole fraction of CO_2 in the gas
y_{in} = mole fraction of CO_2 inlet gas
y_{out} = mole fraction of CO_2 outlet gas

Greek Letters

α = specific area, m^2/m^3
ω = rotating speed, r/min

Abbreviations

MDEA = methyldiethanolamine
R_3N = MDEA
R_3H^+ = protonized MDEA

Literature Cited

(1) Weiland, R. H.; Sivasubramanian, M. S.; Dingman, J. C. Effective Amine Technology: Controlling Selectivity, Increasing Slip, and Reducing Sulfur. *The 53rd Annual Laurence Reid Gas Condition Conference*, Norman, OK,February 2003.

(2) Bucklin, R. W.; Won, K. W. Higee contactors for selective H_2S removal and superdehydration. *Laurance Reid Gas Conditioning Conference*, University of Oklahoma,March 1987.

(3) Stephen, C. S.; Woodcock, K. E.; Meyer, H. S.; Fowler, R. Selective acid gas removal using the Higee absorber. *AIChE Spring Meeting*, Orlando, FL, March 1990.

(4) Donaldson, T. L.; Nguyen, Y. N. Carbon dioxide reaction kinetics and transport in aqueous amine membranes. *Ind. Eng. Chem. Fundam.* **1980**, *19*, 260–266.

(5) Yu, W. C.; Astarita, G.; Savage, D. W. Kinetics of carbon dioxide absorption in solutions of methyldiethanolamine. *Chem. Eng. Sci.* **1985**, *40*, 1585–1590.

(6) Rinker, E. B.; Ashour, S. S.; Sandall, O. C. Kinetics and modelling of carbon dioxide absorption into aqueous solutions of N-methyldiethanolamine. *Chem. Eng. Sci.* **1995**, *50* (5), 755–768.

(7) Ko, J. J.; Li, M. H. Kinetics of absorption of carbon dioxide into solutions of N-methyldiethanolamine+water. *Chem. Eng. Sci.* **2000**, *55*, 4139–4147.

(8) Lu, J. G.; Zheng, Y. F.; He, D. L. Selective absorption of H_2S from gas mixtures into aqueous solutions of blended amines of methyldiethanolamine and 2-tertiarybutylamino-2-ethoxyethanol in a packed column. *Sep. Puri. Tech.* **2006**, *52* (2), 209–217.

(9) Mandal, B. P.; Biswas, A. K.; Bandyopadhyay, S. S. Selective absorption of H_2S from gas streams containing H_2S and CO_2 into aqueous solutions of *N*-methyldiethanolamine and 2-amino-2-methyl-1-propanol. *Sep. Purf. Tech.* **2004**, *35*, 191–202.

(10) Qian, Z.; Guo, K. Modeling study on absorption of CO_2 by aqueous solutions of *N*-Methyldiethanolamine in rotating packed bed. *Ind. Eng. Chem. Res.* **2009**, *48* (20), 9261–9267.

(11) Yu, W. C.; Astarita, G. Design of packed towers for selective chemical absorption. *Chem. Eng. Sci.* **1987**, *42* (3), 425–433.

(12) Mandal, B. P.; Bandyopadhyay, S. S. Simultaneous absorption of carbon dioxide and hydrogen sulfide into aqueous blends of 2-amino-2-methyl-1-propanol and diethanolamine. *Chem. Eng. Sci.* **2005**, *60*, 6438–6451.

(13) Pacheco, M. A.; Rochelle, G. T. Rate-Based Modeling of Reactive Absorption of CO_2 and H_2S intoAqueous Methyldiethanolamine. *Ind. Eng. Chem. Res.* **1998**, *37*, 4107–4117.

(14) Astarita, G.; Savage, D. W.; Bisio, A. *Gas treating with chemical solvents*; Wiley: New York, 1983.

(15) Guo, F.; Zheng, C.; Guo, K. Hydrodynamics and mass transfer in crossflow rotating packed bed. *Chem. Eng. Sci.* **1997**, *52*, 3853–3859.

(16) Yi, F.; Zou, H. K.; Chu, G. W.; Shao, L.; Chen, J. F. Modeling and experimental studies on absorption of CO_2 by Benfield solution in rotating packed bed. *Chem. Eng. J.* **2009**, *145*, 377–384.

(17) Savage, D. W.; Funk, E. W.; Yu, W. C.; Astarita, G. Selective absorption of hydrogen sulfide and carbon dioxide into aqueous solutions of methyldiethanolamine. *Ind. Eng. Chem. Fundam.* **1986**, *25* (3), 326–330.

(18) Lin, C. C.; Liu, W. T.; Tan, C. S. Removal of carbon dioxide by absorption in a rotating packed bed. *Ind. Eng. Chem. Res.* **2003**, *42*, 2381–2386.

(19) Saha, A. K.; Bandyopadhyay, S. S.; Saju, P.; Biswas, A. K. Selective removal of hydrogen sulfide from gases containing hydrogen sulfide and carbon dioxide by absorption into aqueous solutions of 2-amino-2-methyl-1-propanol. *Ind. Eng. Chem. Res.* **1993**, *32* (12), 3051–3055.

(20) Ouwerkerk, C. Design for selective hydrogen sulfide absorption. *Hydrocarbon Process.* **1978**, *57* (4), 89–94.

Received for review March 19, 2010
Revised manuscript received April 26, 2010
Accepted May 3, 2010

IE100678C